Spin-polarized electron momentum density distributions in the Invar system Fe$_3$Pt

J. W. Taylor,[1] J. A. Duffy,[1] A. M. Bebb,[1] J. E. McCarthy,[2] M. R. Lees,[1] M. J. Cooper,[1] and D. N. Timms[3]

[1]*Department of Physics, The University of Warwick, Coventry, CV4 7AL, United Kingdom*
[2]*European Synchrotron Radiation Facility, BP 220, F-38043, Grenoble Cedex, France*
[3]*School of Earth and Environmental Sciences, The University of Portsmouth, Portsmouth, PO1 2DT, United Kingdom*

The one-dimensional projections of the spin polarized electron momentum distributions of Fe$_3$Pt have been measured, using the magnetic Compton scattering technique, in the temperature range 15–500 K, for the 110 and 111 crystallographic directions in the chemically ordered and disordered phases. The experimental data have been compared with results from electronic structure calculations performed using the linearized muffin-tin-orbital and full potential linearized augmented plane-wave methods and the single-site Green's-function Korringa-Kohn-Rostoker method for the ordered and disordered samples, respectively. The projection of the spin moment momentum distribution as a function of temperature remains characteristic of a Fe 3d moment until well above T_c. No evidence of an indicative change in profile shape is observed that would suggest a redistribution of charge from e_g to t_{2g} orbitals in the Fe band structure that would, in turn, support the Weiss two-state model for the Invar effect.

I. INTRODUCTION

The alloy series Fe$_{1-x}$Pt$_x$ exhibits the Invar effect around the ordered crystallographic phase Fe$_3$Pt. A recent investigation by Srajer *et al.*[1] reported a change in the spin-polarized electron momentum distribution at high temperature in the Invar compound Fe$_3$Pt, which may imply a charge transfer between the e_g and t_{2g} Fe d-band orbitals near the Fermi energy.

Much theoretical work has been undertaken on the Invar problem since the phenomenological two-state model was suggested by Weiss.[2] He suggested that in Invar systems there are two nearly degenerate magnetic states: a high-spin, high-volume state, and a low-spin, low-volume state. The relative populations of these states depends upon the system temperature in such a way as to create a large volume magnetostriction that opposes the thermal expansion of the lattice. There has been as yet no experimental evidence that conclusively supports the two state model. It would require some degree of charge transfer between the minority-spin e_g and majority-spin t_{2g} Fe 3d band orbitals near the Fermi energy, in order for the spin state of the Fe sites to change from a high-spin state to a low spin state. Such a charge transfer has been predicted by a number of band-structure calculations.[3]

The experimental work by Srajer *et al.* implies that such a charge transfer may exist in Fe$_3$Pt. However, magnetic form factor measurements as a function of temperature by Brown, Ziebeck, and Neumann,[4] using the spin-polarized neutron-scattering technique on NiFe in the Invar composition, shows no evidence of a charge transfer in the material. Photoemission data[5] that claimed to show evidence of a high-spin to low-spin transition in Fe$_3$Pt were quickly refuted.[6] Furthermore, a recent theoretical calculation,[7] where the nature of the Invar effect was attributed to non-collinearity in the ground-state magnetic structure of the material, was not observed in experiment; indeed NiFe, in the Invar composition, is thought to be a collinear ferromagnet.[8]

A Martensitic phase transition has been observed[9,10] in Fe$_3$Pt, such that the face-centered-cubic lattice transforms to a body-centered-tetragonal (bct) structure below ≈ 100 K. A softening of the transverse acoustic, 110-phonon mode has been observed around this temperature, which in other Martensitic materials has been taken as a precursor signal to the Martensitic transition. This then is clear evidence of strong magnetoelastic coupling in these compounds. It is well known that the structural order in this series strongly influences the magnetism, such that the difference in T_c between ordered and disordered samples is 130 K, with the transition temperatures being 380 and 510 K for the disordered and ordered phases, respectively.

In this paper we report the use of the magnetic Compton scattering technique, to investigate systematically the one-dimensional momentum distribution of the spin moment as a function of temperature, crystallographic direction, and chemical order. Our experimental data are compared with the results from three separate electronic structure calculation methods.

The technique of magnetic Compton scattering samples only the spin moment. After comparison with bulk magnetization measurements, the orbital moment can be deduced, without the necessity of theoretical models. Furthermore the magnetic Compton profile is extremely sensitive to the various interband hybridizations that occur as a result of a local moment in a metallic matrix, since it samples the momentum contributions of all spin-polarized electrons from all bands. Thus the total spin moment is sampled directly. It is therefore an ideal technique for determining if the spin interaction is modeled correctly by theory. The shape of the magnetic Compton profile intrinsically carries information about the overall localization of the moment, as the momentum-space wave function is related to the real-space wave function via a Fourier transform. The ability to comment upon the localization of the spin moment is a useful asset[11] when making comparisons with the theoretical magnetic Compton line shapes, as the localization of the moment and its interaction

with the surrounding conduction electrons, i.e., the *s-d* interaction, is the mechanism which drives the magnetism.

Alloys of the series $Fe_{1-x}Pt_x$ form a congruent solid solution in the compositional range 15–35- at % Pt below 1100 K. A single-crystal sample of Fe_3Pt was grown using the Bridgemann technique from starting materials of at least $4N$ purity. The stoichiometry of the sample was verified using the scanning electron microscopy energy-dispersive x-ray technique. Two thin disk samples (thickness 1 mm) were cut from the original boule along the 110 and 111 crystallographic directions, and the crystallographic order and structure was verified as the Cu_3Au structure using x-ray Laue back-reflection photography. The chemically ordered and disordered samples were produced by furnace annealing at 1000 K for six days followed by a slow cool and a rapid quench, respectively. The magnetic characteristics were verified using vibrating sample magnetometer (VSM) magnetization measurements. The ferromagnetic transition temperatures were measured as 390 and 500 K for the disordered and ordered samples, respectively. The observed ferromagnetic transition temperatures agree well with those found previously, confirming that the samples used for this investigation had the correct chemical order.

II. MAGNETIC COMPTON SCATTERING

The Compton effect is observed when high-energy photons are inelastically scattered by electrons. The scattered photon energy distribution is Doppler broadened, since the electrons have a finite momentum distribution. If the scattering event is described within the impulse approximation[13] the measured Compton spectrum is proportional to the scattering cross section:[14]

The Compton profile is defined as a one-dimensional (1D) projection onto the scattering vector of the electron momentum distribution, $n(\mathbf{p})$, where the scattering vector is taken parallel to the z direction:

$$J(p_z) = \int \int n(\mathbf{p}) dp_x dp_y. \tag{1}$$

The integral of $J(p_z)$ is the total number of electrons per formula unit.

Magnetic Compton scattering (MCS) is a probe which is sensitive to the spin component of a material's magnetization when the scattering event occurs within the impulse approximation. If the incident beam has a component of circular polarization, the scattering cross section contains a term which is spin dependent.[15] In order to isolate the spin dependence one must either flip the sample's direction of magnetization parallel and antiparallel with respect to the scattering vector or "flip" the direction of the photon helicity by 180°. Either method results in a magnetic Compton profile (MCP) $J_{mag}(p_z)$, that is dependent upon only the unpaired spin in the sample, the MCP is defined as the 1D projection of the spin-polarized electron momentum density:

$$J_{mag}(p_z) = \int \int [n^\uparrow(\mathbf{p}) - n^\downarrow(\mathbf{p})] dp_x dp_y. \tag{2}$$

Here $n^\uparrow(\mathbf{p})$ and $n^\downarrow(\mathbf{p})$ are the momentum densities of the majority- and minority-spin bands. The integral of the MCP is the total spin moment per formula unit (FU) in the sample. MCS is an established technique for determining spin-polarized electron densities.[16–18] Within the impulse approximation the method has been shown to be insensitive to the orbital moment.[19] Unlike magnetic x-ray circular dichroism (MXCD),[12] MCS samples all the spin-polarized electrons regardless of their binding energies and wave function symmetries.

III. EXPERIMENT AND DATA ANALYSIS

The magnetic Compton profiles of ordered and disordered Fe_3Pt were resolved along two major crystallographic directions as a function of temperature at the high-energy beamline ID15A at the ESRF. The experiment was performed in reflection geometry as a function of temperature in the range 15–500 K. The temperature controlled sample environment consisted of a closed-cycle He refrigerator fitted with a bifaler wound furnace. An incident beam energy of 220 keV was selected using a Si 311 monochromator in Laue geometry. The spin-dependent signal was isolated by reversing the sample's magnetization vector using a 1T electromagnet. At high photon energies, as were used for this investigation, (desirable for optimum resolution and interpretation within the impulse approximation), reversing the helicity of the incident photons is not yet practical. Circular polarization was produced by selecting a beam approximately 2 μrad below the plane of the electron orbit,[20] this value being chosen to maximize the ratio of magnetic scattering to statistical noise in the charge scattering. A degree of circular polarization of about 45% was obtained. The energy spectrum of the scattered flux was measured using a 13-element Ge detector at a mean scattering angle of 170°. The momentum resolution of the magnetic Compton spectrometer, taken as the full width at half maximum (FWHM) of the instrument response function, was 0.40 a.u. (where 1 a.u. of momentum is defined as 1.99×10^{-24} kg m s^{-1}). The resolution of the spectrometer is determined by the detector collimation, the source divergence, and the intrinsic resolution of the Ge detector. The former are easily determined; the latter, and most important is determined by measurement of the FWHM of the principle emission line of (in this case) Eu^{152} at 121.78 keV, chosen as it coincides in energy with the Compton peak. Thus one has a direct measurement of the detector resolution in the region of interest.

The total number of counts in the charge Compton profiles was 2×10^8, corresponding to a statistical precision of $\pm 2\%$ in the resulting MCP, in a bin width of 0.1 a.u. Since the MCP is the difference between two charge Compton profiles, components arising from spin-paired electrons and from most sources of systematic error are effectively canceled out. The data were corrected for energy-dependent detector efficiency, sample absorption, and the relativistic scattering cross section. The magnitude of the magnetic multiple scattering was determined to be no more than 0.5%. The profiles were corrected for multiple scattering using the technique described by Felsteiner *et al.*[21] After checking that the resulting spectra were symmetric about $p_z = 0$, the profiles

were folded to improve the effective statistics. The profile areas were normalized to an absolute spin scale using Fe data taken under the same conditions.

IV. CALCULATION OF J_{mag} USING THE LINEARIZED MUFFIN-TIN-ORBITAL (LMTO) METHOD

The spin-dependent electron momentum distributions for Fe_3Pt were calculated using the LMTO method within the atomic sphere approximation, including combined correction terms,[22,23] by Major *et al.*[24] The exchange-correlation part of the potential was described in the local-spin-density approximation (LSDA).[25] The self-consistent band structure was solved at 816 k points in the irreducible part of the Brillouin zone (BZ) using a basis set of s-, p-, d-, and f-type wave functions. The Cu_3Au structure was used with a lattice parameter of 7.124 a.u. With these parameters, each Fe carried a moment of $2.624\mu_B$ while the Pt site had a spin-polarized moment of, $0.489\mu_B$, giving a net moment of 2.09 $\mu_B F^{-1}$, where the formula unit F for this composition is taken as $Fe_{0.75}Pt_{0.25}$. The electronic wave functions were then used to generate the electron momentum densities for the spin-up and down bands separately. A total of 3695 reciprocal-lattice vectors were used in the calculation of the momentum density (see also Andersen[22] and Singh and Jarlborg[26]). Double integration of the momentum density results in the theoretical spin-polarized Compton profiles. The theoretical profiles were then convoluted with a Gaussian of 0.4-a.u. FWHM in order to simulate the experimental resolution function, and thus allow a direct comparison with experiment. The theoretical magnetic Compton profile for Fe_3Pt was then produced by taking the difference of the resolution broadened spin-up and -down charge Compton profiles. A full account of their study can be found in Ref. 24.

V. CALCULATION OF J_{mag} USING THE FULL POTENTIAL LINEAR AUGMENTED PLANE-WAVE (FLAPW) METHOD.

A self-consistent potential of ferromagnetic Fe_3Pt was determined by the FLAPW and generalized gradient approximation method coded in WIEN97. The value of the lattice constant a used was 7.086 a.u. The energy values and wave functions were calculated at 253 k points for 1/48 of the BZ. The 253 k points make a cube mesh. In order to determine the eigenfunctions, 300 LAPW's have been used in the expansion of the wave functions outside the muffin-tin spheres (interstitial region), and the wave functions inside a muffin-tin sphere whose radius r_{mt} is 2.4 a.u. were expanded up to $l=10$ for the self-consistent band calculation and $l=4$ for the Compton profiles, where l denotes the angular momentum quantum number.

Compton profiles for Fe_3Pt single crystals were calculated along two major axes 111 and 110, by Wakoh and Tokii,[27] using the band structure determined previously, and integrating $n(\mathbf{p})$ over a series of planes corresponding to different momenta p_z by a linear tetrahedron method.[27] In this regime the Fe spin moment was reported to be $2.771\mu_B$ per atom. The induced spin moment on the Pt site was determined as

$0.364\mu_B$ per atom. This yields a total spin moment of $2.169\mu_B$ per formula unit for $Fe_{0.75}Pt_{0.25}$ The resulting theoretical charge Compton profiles were convoluted with a Gaussian of 0.4-a.u. FWHM to simulate the experimental resolution function, and thus allow a direct comparison with experiment. A full discussion of their investigation can be found in Ref. 27.

VI. CALCULATION OF $J_{mag}(P_z)$ USING THE KOHN-KORRINGA-ROSTOCKER KKR METHOD WITHIN THE COHERENT POTENTIAL APPROXIMATION (KKR-CPA)

The spin-dependent momentum densities of chemically disordered $Fe_{0.75}Pt_{0.25}$ were calculated by Major *et al.*[24] using the KKR Green's-function method[28–30] within the coherent potential approximation (CPA) (Refs. 31–33) and using muffin-tin potentials. Self-consistency was achieved using an adaptive mesh of k points determined by the required integration tolerances.[34] The averaging over the disorder is done adequately by the coherent potential approximation. The approach has been to calculate the momentum density $n(\mathbf{p})$ and integrate directly around a contour in the complex energy plane. The isotropic potentials are placed onto crystal lattice structure which in turn invokes directional anisotropies in the calculated wave-functions. The exchange-correlation component of the potential was described in the LSDA.[25] The method were described more fully elsewhere.[24,35] The momentum density is given, in terms of the Greens function $G(\mathbf{p},z)$ by

$$n(\mathbf{p}) = -\int \frac{dE}{\pi} f(E) \text{Im}\, G[(\mathbf{p});E+i\,\eta], \qquad (3)$$

where E is real and $f(E)$ denotes the Fermi factor (our calculations are done at a finite temperature).

Double integration of the momentum density $n(\mathbf{p})$ along the crystallographic direction results in the determination of the charge Compton profile $J(p_z)$. The solid solution of Pt in Fe was simulated using a disordered arrangement of atoms on a fcc lattice with spacing 7.124 a.u. for $Fe_{0.75}Pt_{0.25}$. The directional charge Compton profiles (including contributions from the core and valence electrons) behaved as expected in the large momentum region of the profile, showing a monotonic decrease to zero. A similar calculation was performed for pure Fe, i.e., $Fe_{0.75}Fe_{0.25}$ on the same fcc lattice for comparison.

In this regime the Fe spin moment was determined to be $2.737\mu_B$ per atom. The induced spin moment on the Pt site was determined as $0.324\mu_B$ per atom. This yields a total spin moment of $2.136\mu_B$ per formula unit for $Fe_{0.75}Pt_{0.25}$ Again the resulting theoretical charge Compton profiles were convoluted with a Gaussian of 0.4-a.u. FWHM to simulate the experimental resolution function and thus allow a direct comparison with experiment. The theoretical spin-polarized electron momentum distribution were calculated in the same manner as previously described.

TABLE I. Experimental and calculated spin moments for ordered and disordered $Fe_{0.75}Pt_{0.25}$. Results are quoted as μ_B per formula unit of $Fe_{0.75}Pt_{0.25}$. The spin moment per Fe atom is shown in brackets. (For the experimentally determined values we assume that there is a negligible spin polarized contribution from Pt.)

	Ordered sample	Disordered sample
15 K MCS spin moment	1.85 ±.02 (2.46)	1.64±.02 (2.18)
300-K MCS spin moment	1.54± .02 (2.056)	1.47±.02 (1.97)
300-K VSM total moment	1.61 (2.16)	
KKR spin moment		2.136 (2.73)
LMTO spin moment	2.096 (2.62)	
FLAPW spin moment	2.169 (2.77)	

VII. RESULTS

The theoretical and measured spin moments are compared in Table I. Moments are presented as per formula unit (FU^{-1}) of $Fe_{0.75}Pt_{0.25}$. It is clear that the spin moment is overestimated by all three methods of calculation. The experimental spin moments and the measured total moments (measured using a VSM) compare well to those expected for the spin moment and the total moment in Fe (assuming that there is negligible Pt spin polarization in the system). The low-temperature (15 K) spin moments are higher than one may expect for Fe, that is to say that the spin moment per Fe atom is greater that $2.05\mu_B$. This possibly arises from the bct distortion in Fe_3Pt at 100 K inducing a finite polarization on the Pt bands.

A. Ordered Fe_3Pt

The one-dimensional projection of the spin moment momentum distribution for ordered Fe_3Pt resolved along the 110 and 111 directions at 300 K are shown in Figs. 1 and 2.
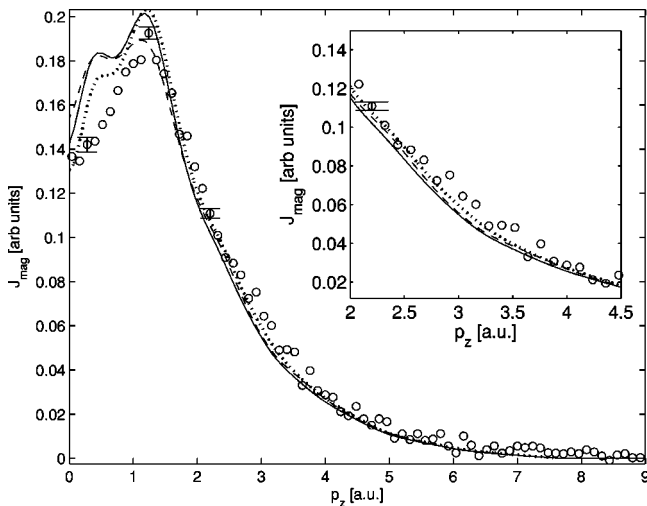

FIG. 1. The experimental MCP at 300 K (circles) and calculated, LMTO (full line), and FLAPW (dotted) for Fe_3Pt resolved along the 110 crystallographic direction. The dashed line indicates the calculated magnetic profile for pure Fe on a fcc lattice. For the purposes of comparison data are normalized to have equal areas. The inset shows the same data in the region of 2–4.5 a.u.
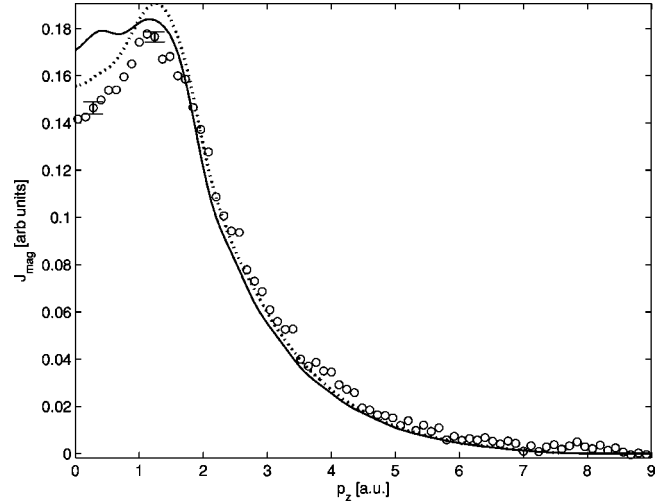

FIG. 2. The experimental MCP at 300 K (circles) and calculated, LMTO (full line), and FLAPW (dotted) for Fe_3Pt resolved along the 111 crystallographic direction. For the purposes of comparison the data are normalized to have equal areas.

The experimental data are compared with the results from LMTO and FLAPW calculations in both cases.

First we shall consider the 110 crystallographic direction (Fig 1). The calculated MCP is in good overall agreement with that measured experimentally; the high-momentum tails of the experimental profiles (above 7 a.u.) are well matched by that calculated theoretically in that both the experiment and the calculated profiles mutually go to zero as expected (the profiles are truncated to a region of interest of 0 to 9 a.u. The tails are not shown). However the FLAPW calculation produces a more realistic MCP in both crystallographic directions in the momentum region below 4 a.u. (see Figs. 1 and 2), as one may expect from a full potential code. It is interesting to note that the calculated spin moments from each calculation (LMTO and FLAPW) are similar (see Table I).

The LMTO calculation was used to create a Fe-only MCP, that is to say Fe_3Fe (with the same lattice parameter as the Fe_3Pt calculation), which is shown by the dashed line in Fig. 1. From this one may conclude that the amount of d band Pt spin polarization calculated in the Fe_3Pt calculation is too great (see Table II), since the Fe only calculation produces a slightly better line-shape comparison, especially in the region corresponding to the d-band contribution to the MCP i.e. from 2 to 4 a.u. (see the inset to Fig. 1).

The situation is similar when one considers the results for the 111 crystallographic direction (Fig. 2); again the full potential code gives a slightly better MCP line shape, when compared with the experimental MCP. For the 111 direction the low-momentum region, i.e., $p_z < 2$ a.u. of the LMTO-calculated MCP is too large; thus the calculation overestimates the amount of delocalized spin polarization in this direction. The full potential code again provides a more realistic comparison with experiment. It is interesting to note that the LMTO code systematically underestimates the spin polarization in the higher-momentum region of the profile and overestimates the spin polarization in the low-

TABLE II. Site spin polarizations in Bohr magnetons, sp-like band components, and d-like band components from LMTO, FLAPW, and KKR calculations of Fe_3Pt. * Denotes an interstitial moment.

	Fe site	Pt site	Fe d-like component	Fe sp-like component	Pt d-like component	Pt sp-like component
LMTO	2.624	0.489	2.632	-0.0183	0.562	-0.0837
FLAPW	2.771	0.364		-0.182*		
KKR-CPA	2.798	0.227				

momentum region of the profile. One possible reason for this is the over estimation of the Pt d-band contribution. A summary of the band and site spin polarizations is given in Table II.

B. Disordered Fe_3Pt

The one-dimensional projections of the spin moment momentum distribution for disordered Fe_3Pt resolved along the 110 and 111 directions at 300 K are shown in Figs. 3 and 4. The experimental data are compared with the results from KKR-CPA calculations in both cases. The calculated MCP is again in good overall agreement with that measured experimentally. The KKR-CPA calculation was used to create a Fe-only MCP, i.e., Fe_3Fe with the same lattice parameter as the Fe_3Pt calculation, which is shown as the dashed line in Figs. 3 and 4. The situation with the disordered calculation is similar to that in the ordered sample (see Sec. VII A), in that the d band region of the profile is underestimated, with an overestimation in the low-momentum region of the profile, corresponding to the delocalized component.

C. Comparison of J_{mag} between ordered and disordered Fe_3Pt

It is interesting to note that the experimental MCP data for the disordered sample look similar to those for the ordered sample. We shall now consider the directional and order/disordered anisotropies. The anisotropy between the ordered and disordered Fe_3Pt resolved along the 110 direction, that is to say the difference between the two MCP's i.e., $\Delta J = J_{mag\,110}^{ordered} - J_{mag\,110}^{disordered}$, is shown in the inset to Fig. 5, along with that predicted by calculation. It is clear from both the main and inset figures that there is very little observed difference in the MCP between the ordered and disordered samples. The calculated differences are of the same order as those which are measured. Thus the measured projection of the spin moment momentum distribution is very similar for the ordered and disordered samples within our resolution when resolved along the directions measured. This is an interesting result since the bulk properties of the material vary greatly with the order present in the sample, as demonstrated in Fig. 6, which shows the low-field magnetization as a function of temperature. Clearly there is, as expected for Fe_3Pt, a large difference in T_c between the ordered and disordered samples.

D. Directional anisotropy of the 111 and 110 directional MCP's of Fe_3Pt

The amount of directional anisotropy between the 110 and 111 directions is clearly small. The directional anisotropy between the 111 and 110 crystallographic directions, i.e.,
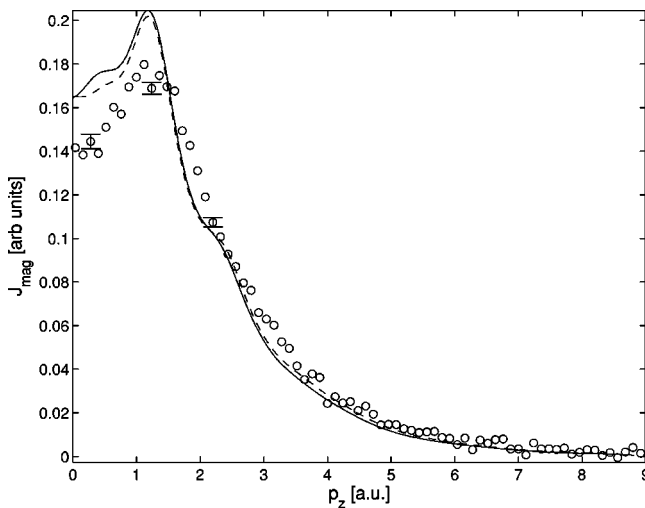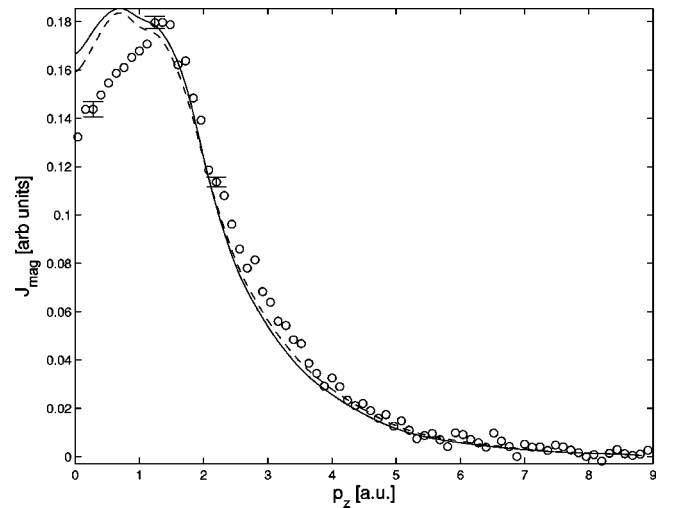

FIG. 3. The experimental MCP at 300 K (circles) and calculated KKR (full line) for disordered Fe_3Pt resolved along the 110 crystallographic direction. The dashed line indicates the calculated magnetic profile for pure Fe on a fcc lattice (data are normalized to have equal areas to aid comparison).
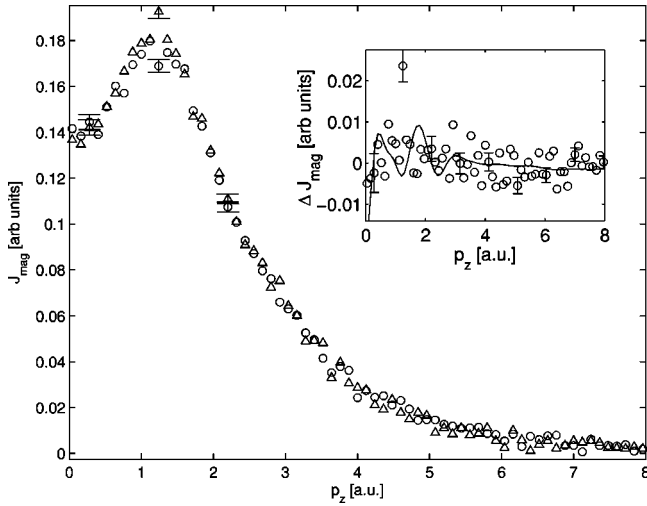

FIG. 4. The experimental MCP at 300 K (circles) and calculated KKR (full line) for disordered Fe_3Pt resolved along the 111 crystallographic direction. The dashed line indicates the calculated magnetic profile for pure Fe on a fcc lattice (data are normalized to have equal areas to aid comparison).

FIG. 5. The experimental MCP for ordered Fe_3Pt (circles) and disordered Fe_3Pt (triangle) resolved along the 110 crystallographic direction. The inset indicates the observed anisotropy between the two profiles compared with that calculated, i.e., the anisotropy between the LMTO and KKR-CPA results along the same direction.

FIG. 7. The experimental MCP for ordered Fe_3Pt resolved along the 111 direction (triangles) and the 110 direction (circles). The inset shows the observed directional anisotropy for the 111-110 directions (circles) and the calculated directional anisotropy from the LMTO calculation.

$\Delta J = J_{mag111} - J_{mag110}$, is shown in the inset to Fig. 7 for the ordered sample together with that calculated from the LMTO band-structure results. The main figure illustrates that there is very little directional anisotropy between these two directions in Fe_3Pt. Again the calculated MCP provide, the correct crystallographic anisotropy when compared with experiment. The overall magnitude of the anisotropy is small, and correctly modeled by the calculations. It is clear from the systematic comparisons of the MCP that for this material there is little difference in the directional profiles see insets to Fig. 7. From the inset to Fig. 5 it is clear that there is no observed difference as a function of order in Fe_3Pt.

The MCP seems insensitive to the degree of order in the samples. The actual degree of order in the samples were confirmed by measurement of the Curie temperatures in the ordered and disordered crystals. The low-field magnetization
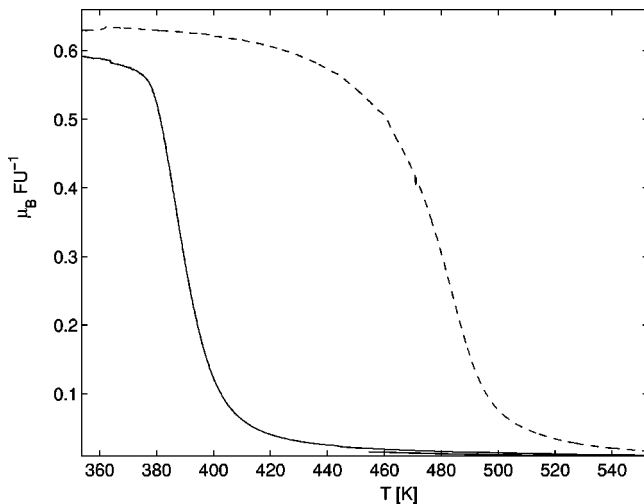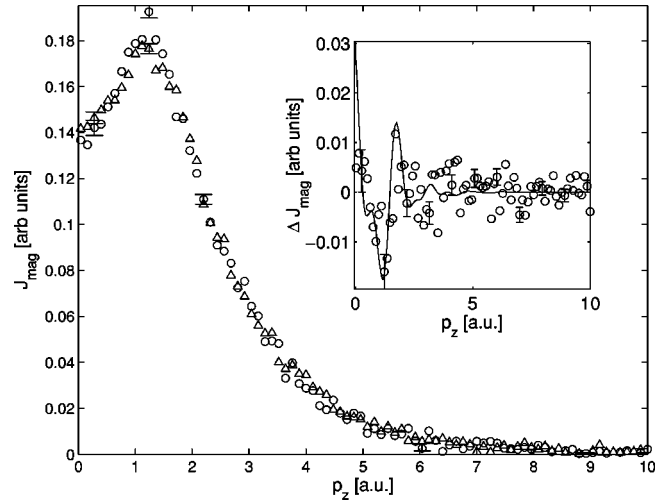
as a function of temperature is shown in Fig. 6 for the ordered and disordered samples; the field was applied parallel to the 111 (easy) direction of the crystal. The measured T_c of the ordered and disordered samples are in good agreement with those measured previously.

E. Temperature dependence of the projection of the spin moment momentum distribution in ordered and disordered Fe_3Pt

The MCP resolved along the 110 direction of the disordered sample, measured at four temperatures, is shown in Fig. 8. It is clear that there is a finite spin moment above T_c in this system, which is commensurate with the presence of short range order correlations in the sample. The inset to Fig. 8 shows the same data normalized such that each profile has the same area. The same result was gained when measuring the MCP as a function of temperature in the ordered sample (see Fig. 9), except here the maximum temperature measured was 500 K. It is clear from this that the spin moment remains wholly Fe in character with no characteristic changes in the 1D spin-polarized electron momentum distribution, as suggested previously in either the ordered or disordered sample. The large amount of scatter in the 425-K data set results from the small net moment that is present above T_c at 425 K caused by the aforementioned short-range order in the sample.

VIII. DISCUSSION

A number of conclusions can be drawn from our results. The measured projections of spin moment momentum distribution are insensitive to the degree of order in the sample, whereas bulk parameters such as T_c are not; that is to say there is very little difference in the MCP observed between the ordered and disordered sample (see Fig. 5). There is very little observed anisotropy between the 111 and 110 crystal-
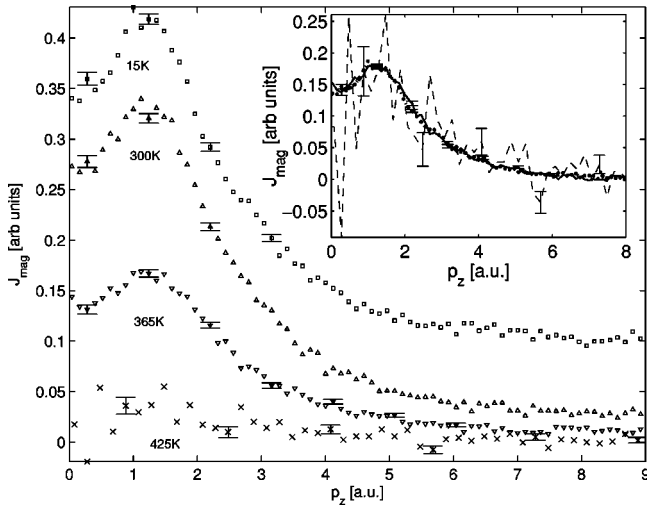

FIG. 6. Low-field magnetization as a function of temperature for ordered (dashed) and disordered (solid) Fe_3Pt.

FIG. 8. The magnetic Compton profile at various temperatures for disordered Fe_3Pt resolved along the 110 direction. The data are offset from zero to aid viewing. The inset shows three 300 (solid), 365 (dotted), and 425 K (dashed) of the profiles with integrated areas of one to aid line shape comparison. Clearly the line shape of the MCP remains constant. The ordered sample Fe_3Pt was also measured in the temperature range from 15 to 500 K, the data show the same trend as illustrated with no change in the MCP line shape.

lographic directions, as predicted by calculation. As a function of temperature there is no discernable (within our resolution) change in the character of the spin moment momentum distribution for either the ordered or disordered samples (see Figs. 8 and 9). The theoretical models used, not only reproduce the MCP line shape reasonably well but also the anisotropic difference profile; however, there is in gen-
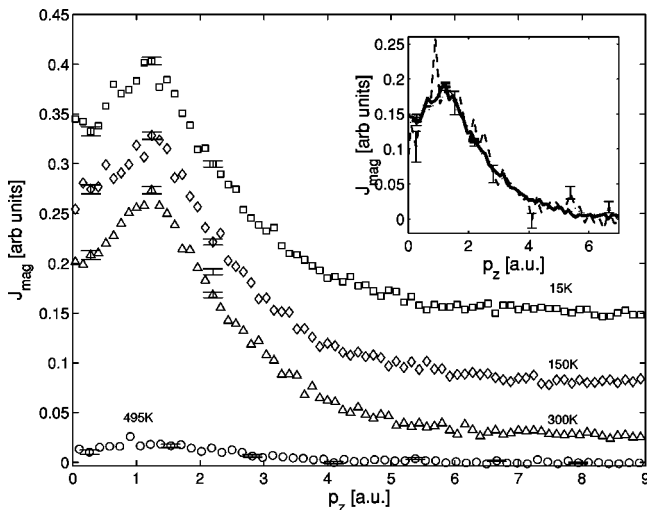

FIG. 9. The magnetic Compton profile at various temperatures for ordered Fe_3Pt resolved along the 110 direction. The data are offset from zero to aid viewing. The inset shows three 15 (solid), 300 (dotted), and 495 K (dashed) of the profiles with integrated areas of 1 to aid line shape comparison. Clearly the line shape of the MCP remains constant. The ordered sample Fe_3Pt was also measured in the temperature range 15 to 500 K; the data show the same trend, as illustrated by no change in the MCP line shape.

eral a $\approx 10\%$ discrepancy between the measured and calculated spin moments. Some possible reasons for these observations will now be discussed.

Our data provide no evidence for a charge transfer between the minority-spin e_g and majority-spin t_{2g} Fe d-band orbitals near the Fermi energy, within the experimental resolution. The magnetic Compton profile is sensitive to all spin-polarized electrons in the system, and is also sensitive to their respective localizations. As the real-space and momentum-space wave functions are related by Fourier transform, spin-polarized electrons that are well localized are manifest as broad features in the MCP, and vice versa. Since the e_g electrons contain a greater delocalized character than those in the t_{2g} orbital, the magnetic Compton technique is sensitive to the respective populations of each orbital.[36]

The fact that we observe no change in the MCP line shapes in ordered and disordered samples between 15 and 500 K is in contrast to the data of Srajer *et al.*[1] who observed a marked change in MCP line-shape for ordered Fe_3Pt between 305 and 490 K. However, our data exhibit no changes in line shape as a function of temperature in the low-momentum region of the profile that would indicate a change in the population of the e_g orbital. On the contrary, the data shown in Fig. 9, when normalized to the same integrated area (see the figure inset) have the same line shapes within experimental error. For both samples, the statistical accuracy is sufficient for this to be well established below T_C. Just above T_C the magnetization density induced by the 1 T applied field appears unchanged in distribution. The same zero effect is observed in the ordered sample as a function of temperature up to 500 K. We also note that independent confirmation of the validity of our data is provided by the fact that, the magnetic moments as calculated from our MCP's (the integrated area under the profile) agree well with those measured using a VSM at all temperatures. Hence, despite the apparent contradiction, we are confident in the validity and interpretation of our data.

From our results it is clear that the full potential code gives a slightly better result that the LMTO and KKR methods. The fact that the lattice parameters vary by $\approx 1\%$ will only effect the calculated spin moment and not the profile shape. If the Fe-only profile is examined for the LMTO result, for example, it is clear that the agreement with the experimental data is somewhat improved. This is an indication that the degree of Pt polarization is overestimated. Now if one examines the site Pt moments for the various calculations (see Table II) the full potential code yields a slightly smaller Pt site moment, which may account for the differences in profile shape. The differences between the calculated and measured spin and total moments (see Table I) has been seen before in Ni (Ref. 37) and in Fe_3Si.[38] The differences between the measured and calculated spin moments are similar in all cases, and an indication that the LSDA is a reasonable approximation to use for the exchange correlation. It is interesting to note that the FLAPW-GGA calculation is no real improvement on the total measured spin moment, but does improve the calculated momentum distribution of the spin moment.

IX. SUMMARY

Our results show that the measured projections (111 and 110) of the spin moment momentum distribution remain constant as a function of temperature in ordered and disordered Fe$_3$Pt; this in turn indicates that no charge transfer occurs between orbitals. This is direct experimental evidence that does not agree with the Weiss two-state model proposed as a possible mechanism behind the Invar effect. The results from three separate electronic structure calculations have been compared with the experimental results. We find good agreement with the profile shape for Fe$_3$Pt in both the ordered and disordered phases, although the calculated spin moments deviate from those measured by $\approx 10\%$.

[1] G. Srajer, C. J. Yahnke, D. R. Haeffner, D. M. Mills, L. Assoufid, B. N. Harmon, and Z. Zuo, J. Phys.: Condens. Matter. **11**, L253 (1999).

[2] R. J. Weiss, Proc. R. Soc. London, Ser. A **82**, 281 (1963).

[3] P. Entel, H. C. Herper, E. Hoffmann, G. Nepecks, E. F. Wassermann, M. Acet, V. Crisan, and H. Akai, Philos. Mag. B **80**, 141 (2000).

[4] P. J. Brown, K. R. A. Zeibeck, and K. U. Neumann, J. Phys.: Condens. Matter **13**, 1563 (2001).

[5] E. Kisker, E. F. Wassermann, and C. Carbone, Phys. Rev. Lett. **58**, 1784 (1987).

[6] Y. Kakehashi, Phys. Rev. B **38**, R12 051 (1988).

[7] M. van Schilfgaarde, I. A. Abrikosov, and B. Johansson, Nature (London) **400**, 46 (1999).

[8] A. Wildes and N. Cowlam (private communication).

[9] K. Tajima, Y. Endoh, and Y. Ishikawa, and W. G. Stirling, Phys. Rev. Lett. **37**, 519 (1976).

[10] J. Kastner, J. Neuhaus, E. F. Wassermann, W. Petry, B. Hennion, and H. Bach, Eur. Phys. J. B **11**, 75 (1999).

[11] J. W. Taylor, J. A. Duffy, A. M. Bebb, M. J. Cooper, S. B. Dugdale, J. E. McCarthy, D. N. Timms, D. Greig, and Y. B. Xu, Phys. Rev. B **63**, 220404(R) (2001).

[12] B. T. Thole, P. Carra, F. Sette, and G. van der Laan, Phys. Rev. Lett. **68**, 1943 (1992).

[13] P. M. Platzman and N. Tzoar, Phys. Rev. **2**, 3556 (1970).

[14] P. Holm, Phys. Rev. A **37**, 3706 (1988).

[15] F. Bell and J. Felsteiner, Phys. Rev. A **53**, R1213 (1996).

[16] J. A. Duffy, S. B. Dugdale, J. E. McCarthy, M. A. Alam, M. J. Cooper, S. B. Palmer, and T. Jarlborg, Phys. Rev. B **61**, 14331 (2000).

[17] J. E. McCarthy, J. A. Duffy, C. Detlefs, M. J. Cooper, and P. C. Canfield, Phys. Rev. B **62**, R6073 (2000).

[18] J. A. Duffy, J. E. McCarthy, S. B. Dugdale, V. Honkimki, M. J. Cooper, M. A. Alam, T. Jarlborg, and S. B. Palmer, J. Phys.: Condens. Matter. **10**, 10391 (1998).

[19] P. Carra, M. Fabrizio, G. Santoro, and B. T. Thole, Phys. Rev. B **53**, R5994 (1996).

[20] J. E. McCarthy, M. J. Cooper, P. K. Lawson, D. N. Timms, S. O. Manninen, K. Hamalainen, and P. Suortti, J. Synchrotron Radiat. **4**, 102 (1997).

[21] J. Felsteiner, P. Pattison, and M. J. Cooper, Philos. Mag. **30**, 537 (1974).

[22] O. K. Andersen, Phys. Rev. B **12**, 3060 (1975).

[23] T. Jarlborg and G. Arbman, J. Phys. F: Met. Phys. **7**, 1635 (1977).

[24] Zs. Major, S. B. Dugdale, T. Jarlborg, E. Bruno, B. Ginatempo, E. S. Giuliano, J. B. Staunton, and J. Poulter (unpublished).

[25] O. Gunnarsson and B. I. Lundqvist, Phys. Rev. B **13**, 4274 (1976).

[26] A. K. Singh and T. J. Jarlborg, J. Phys. F: Met. Phys. **15**, 727 (1985).

[27] S. Wakoh and M. Tokii (unpublished).

[28] J. Korringa, Physica (Amsterdam) **13**, 392 (1947).

[29] W. Kohn and N. Rostoker, Phys. Rev. B **94**, 1111 (1954).

[30] J. S. Faulkner, J. Phys. C **10**, 4661 (1977).

[31] P. Soven, Phys. Rev. B **156**, 809 (1967).

[32] G. M. Stocks, W. M. Temmerman, and B. L. Gyorffy, Phys. Rev. Lett. **41**, 339 (1978).

[33] D. D. Johnson, D. M. Nicholson, F. J. Pinski, B. L. Gyorffy, and G. M. Stocks, Phys. Rev. B **41**, 9701 (1990).

[34] E. Bruno and G. Ginatempo Phys. Rev. B **55**, 12946 (1997).

[35] J. Poulter and J. B. Staunton, J. Phys. F: Met. Phys. **18**, 1877 (1988).

[36] A. Koizumi, S. Miyaki, Y. Kakutani, H. Koizumi, N. Hiraoka, K. Makoshi, N. Sakai, K. Hirota, and Y. Murakami, Phys. Rev. Lett. **86**, 5589 (2001).

[37] M. A. G. Dixon, J. A. Duffy, S. Gardelis, J. E. McCarthy, M. J. Cooper, S. B. Dugdale, T. Jarlborg, and D. N. Timms, J. Phys.: Condens. Matter **10**, 2759 (1998).

[38] E. Zukowski, A. Andrejczuk, L. Dobrzynski, S. Kaprzyk, M. J. Cooper, J. A. Duffy, and D. N. Timms, J. Phys.: Condens. Matter **12**, 7229 (2000).